Polarizable Model Potential Function for Ion−Methanol Systems

Setsuko Nakagawa[†]

Kinjo Gakuin University, Omori, Moriyama-ku, Nagoya 463-8521, Japan

Received: September 2, 1999; In Final Form: January 28, 2000

A polarizable model potential (PMP) function for methanol and three ions (Cl^-, Na^+, and Mg^{2+}) is developed on the basis of high-level ab initio molecular orbital calculations (MP2/6-311++G(2d,2p)). The PMP function consists of Coulomb, polarization, and Lennard-Jones terms. The permanent partial charge parameters of the Coulomb term, and the multicenter polarizability parameters of the polarization term, are determined by using electrostatic potential optimization, and polarizable one-electron potential (POP) optimization, respectively. The Lennard-Jones parameters are adjusted to reproduce the ab initio potential energy surfaces of methanol dimer and ion−methanol complexes. The PMP function using the final parameters reproduced well the ab initio energy surfaces of methanol dimer, ion−methanol, and methanol−ion−methanol systems. The root-mean-square (rms) deviations of ion−methanol systems having various conformations are only 10−12% of the ab initio interaction energies. The electron density changes by the complex formations were reproduced well. The rms deviations are 1−2% of the surface electrostatic potentials. The interaction energies of each classical term were compared with the corresponding terms derived from an ab initio energy decomposition analysis (EDA). The Coulomb and polarization energy reproduced well the electrostatic and induction energy of EDA, respectively. The Lennard-Jones energy reproduced well the sum of EDA exchange repulsion energy, dispersion energy, and deformation energy. In the PMP function, most many-body effects can be adequately evaluated by the introduction of multicenter polarizabilities determined from the POP optimization.

Introduction

For the last 2 decades, classical simulations of molecular systems using pairwise additive potentials have been successfully applied to investigate the structures and thermodynamics of solutions[1−6] and biological systems.[7−9] In the pair potentials it had been supposed that many-body effects are negligible or incorporate into effective pair potentials, in which the parameters of the potentials are optimized to the experimental observations by averaging.[4−6] However, it has been recognized that the introduction of many-body effects is indispensable to construct potentials suited both to isolated small clusters and to the condensed phase.[10] Most of the many-body effects might be taken into account through molecular polarization.[11] Inclusion of the polarization effects is presumed to be significant for describing the energetics of cluster chemistry, ionic solvation, and interfacial phenomena.

The polarization term has been explicitly introduced into the potential functions in recent molecular simulations of water cluster, ion−water cluster, liquid water, ion solvation, aqueous solution, and water interface. A variety of water polarization models, namely, single isotropic polarizability,[10,12−15] fluctuating charges,[16,17] atomic polarizabilities,[18−23] and bond polarizabilities,[24,25] have been used for those simulations. The single polarizability might be appropriate for water molecules showing a small polarization anisotropy. However, it is difficult to depict the polarization response of larger molecules under strongly nonuniform external fields. Empirical atomic polarizabilities or site polarizabilities have often been used for molecular simulations in order to introduce more detailed polarization.[26−29] The introduction of such polarization models is relatively easy for molecular simulations, and the empirical parameters are available from the professional literature.[30−32] However, the introduction of the empirical polarizabilities should be examined, because the empirical method is an approximation for rationalizing and predicting dielectric properties rather than the microscopic electronic response.

Much effort has gone into calibrating polarizable potential functions from accurate ab initio molecular orbital (MO) calculations.[33,34] The ab initio calculations have been used not only for the potential energy surfaces of interacting molecules but also for the determination of distributed polarizabilities. The distributed polarizabilities can be extracted directly from the ab initio coupled perturbed Hartree−Fock (CPHF) or finite field Hartree−Fock method,[35−37] or they can be chosen to reproduce the dipole polarizability of molecule.[38] Several partitioning schemes have been proposed for molecular polarizability,[39,40] and the distributed polarization parameters have been applied to the molecular simulations.[41]

As opposed to these approaches based on molecular polarizability, it is possible to determine directly the apparent multicenter polarizabilities from the changes of electron densities.[42−44] The variations of electrostatic potentials on the molecular surface induced by a external field point charge can be reproduced by the optimization of classical multicenter polarizabilities such as atomic and bond polarizabilities. The field point charge, which is placed on an appropriate molecular surface, represents a strongly nonuniform external field induced by a nearby ion. The variations of electrostatic potentials are called polarized one-electron potentials (POP). The POP optimization has been applied to water, hydrocarbons, alcohol, and benzene, and it was shown that the microscopic electron redistribution is well reproduced by the classical polarizabilities.[42−44]

A goal of present work is to provide a reliable procedure

[†] E-mail: naka@kinjo-u.ac.jp. Fax: +81−52−798−0370.

10.1021/jp993124a CCC: $19.00
Published on Web 05/13/2000

which gives the parameters of the polarizable potential function for the molecular simulations of inhomogeneous condensed systems including ions. The methanol molecule is chosen for the test case, because the polarization anisotropy of methanol ($\alpha_1 = 21.8$ au, $\alpha_2 = 17.9$ au, $\alpha_3 = 27.6$ au) is larger than that of water ($\alpha_1 = 10.3$ au, $\alpha_2 = 9.5$ au, $\alpha_3 = 9.9$ au).[45,46] Three ions of Cl^-, Na^+, and Mg^{2+} are chosen in order to test the electric response of methanol under various strong electric fields. The polarizable model potential (PMP) function studied here consists of Coulomb, polarization, and Lennard-Jones (LJ) terms. Especially the parameters of polarization term are definitely determined by the POP optimization. The interaction energy reproductions of methanol dimer, of ion−methanol, and of methanol−ion−methanol systems are evaluated using the high-level molecular orbital calculations. In the following, details of computational methods and parametrization are described. Then, results and discussions for the reproducibility of energy surfaces and for the energy term analysis are presented.

Methods

Polarizable Model Potential Function. The total energy of an interacting molecular system is given below, and consists of a electrostatic term (E_{es}), a van der Waals term (E_{vdw}), and a polarization term (E_{pol}):

$$E_{tot} = E_{es} + E_{vdw} + E_{pol} \tag{1}$$

In eq 1, the terms of electrostatic and van der Waals are pairwise additive, but the polarization term is nonadditive.

The electrostatic energy between molecules A and B is determined by the following Coulombic form:

$$E_{es} = \sum_{i}^{onA} \sum_{j}^{onB} \frac{q_i q_j}{R_{ij}} \tag{2}$$

Here, R_{ij} is the distance between sites i and j, and q_i is the permanent partial charges on site i. Intramolecular charge−charge interactions are not taken into account.

The van der Waals interaction energy between molecules A and B is determined by the Lennard-Jones potential:

$$E_{vdw} = \sum_{i}^{onA} \sum_{j}^{onB} \epsilon_{ij} \left[\left(\frac{R^*_{ij}}{R_{ij}} \right)^{12} - 2 \left(\frac{R^*_{ij}}{R_{ij}} \right)^{6} \right] \tag{3}$$

Here R_{ij} is the distance between atomic sites i and j, and R^*_{ij} and ϵ_{ij} are formed from the intrinsic atom parameters R^*_i, R^*_j, ϵ_i, and ϵ_j. Standard combination rules such as $R^*_{ij} = R^*_i + R^*_j$ and $\epsilon_{ij} = (\epsilon_i \epsilon_j)^{1/2}$ are used to determine the R^*_{ij} and ϵ_{ij}.

The polarization energy is expressed as follows:

$$E_{pol} = -\frac{1}{2} \sum_{i}^{N} \Delta\mu_i \, \mathbf{F}_i^{\mathbf{0}} \tag{4}$$

where $\Delta\mu_i$ is the induced dipole moment of site i, and $\mathbf{F}_i^{\mathbf{0}}$ is the electrostatic field at site i due to the permanent charges of all other sites belonging to different molecules. The induced dipole moments are calculated self-consistently as follows:

$$\Delta\mu_i = \alpha_i \left(\mathbf{F}_i^{\mathbf{0}} - \sum_{j \notin a(i)} \tilde{\mathbf{T}}_{ij} \Delta\boldsymbol{\mu}_j \right) \tag{5}$$

where α_i is the polarizability of site i and the expression $j \notin a(i)$ indicates that site j is not in the molecule containing site i. Thus, intramolecular polarization is not taken into account. The dipole field tensor is given as follows:

$$\tilde{\mathbf{T}}_{ij} = \frac{1}{r_{ij}^3} \left(\tilde{\mathbf{1}} - \frac{3\mathbf{r}_{ij} \otimes \mathbf{r}_{ij}}{r_{ij}^2} \right) \tag{6}$$

An iterative procedure is used to solve eq 5. Convergence is achieved when the deviation of the induced dipole moments from two sequential iterations falls to within 0.000025 D/site.

Parametrization. The electrostatic potential (ESP) optimization method has been widely used to determine the partial charges of molecules.[47,48] The electrostatic potentials ($V^{QM}(R_l)$) at several points on an appropriate molecular surface are evaluated from the wave function of an isolated molecule and are used as the reference of the charge optimization. The electrostatic potential is rigorously defined by the quantum mechanical expression value of the operator r^{-1},

$$V^{QM}(\mathbf{R}_l) = \sum_i \frac{Z_i}{|\mathbf{R}_l - \mathbf{R}_i|} - \int \frac{\rho(\mathbf{r})}{|\mathbf{R}_l - \mathbf{r}|} \, d\mathbf{r} \tag{7}$$

where the first term represents the electrostatic contribution from the nuclear charges Z_i located at positions $\mathbf{R}_i$. The second term in eq 7 represents the electrostatic potential originating from the electron density $\rho(r)$ throughout the whole space. In the electrostatic potential evaluation, the wave function is not perturbed by the external field; that is, the wave function under the unperturbed Hamiltonian (H°) is kept frozen (ψ^0) even under the perturbed Hamiltonian ($H^\circ + H^k$). The reference electrostatic potentials of methanol are estimated from the MP2/6-311++G(2d,2p) wave function.

In the classical picture, the electron density is approximated by discrete point charges (q_i). The classical electrostatic potential is given as follows:

$$V^{CM}(\mathbf{R}_l) = \sum_i \frac{q_i}{|\mathbf{R}_l - \mathbf{R}_i|} \tag{8}$$

The electrostatic potentials defined in eqs 7 and 8 are estimated on the molecular surface determined by an envelope of 1.8 times the van der Waals radius of the atoms. A nonlinear optimization procedure is used to minimize the following target function in order to determine the fractional point charges:

$$\chi^2 = \sum_l^L [V^{CM}(\mathbf{R}_l) - V^{QM}(\mathbf{R}_l)]^2 \tag{9}$$

The polarized one-electron potential (POP) optimization method[42−44] is used to determine the multicenter polarization of methanol. To evaluate the polarization effect, it is necessary to relax the wave function (ψ_k) under the perturbed Hamiltonian ($H_0 + H_k$). When a molecule is polarized, the one-electron potential is modified. In quantum mechanics, we can evaluate the change in the one-electron potential ($V_k^{QM}(\mathbf{R}_l)$) by the polarization as follows:

$$\Delta V_k^{QM}(\mathbf{R}_l) = \int \frac{\Delta\rho_k(\mathbf{r})}{|\mathbf{R}_l - \mathbf{r}|} \, d\mathbf{r} \tag{10}$$

where $\Delta\rho_k(\mathbf{r})$ is the difference between the electron densities obtained from the frozen and relaxed wave functions (ψ_0 and ψ_k).

On the other hand, in the classical picture, the difference is approximated as several discrete fractional charges (Δq_{ki}). Then,

the multicenter expansion of the potential change is given as follows:

$$\Delta V_k^{\mathrm{CM}}(\mathbf{R}_l) = \sum_i \frac{\Delta q_{ki}}{|\mathbf{R}_l - \mathbf{r}_i|} \tag{11}$$

A nonlinear optimization procedure is used to minimize the following quantity in order to determine the induced dipoles:

$$\chi^2 = \sum_j^J \sum_k^K \sum_l^L [\Delta V_{jk}^{\mathrm{CM}}(\mathbf{R}_l) - \Delta V_{jk}^{\mathrm{QM}}(\mathbf{R}_l)]^2 \tag{12}$$

A field point charge is placed on the molecular surface defined by an envelope of 1.8 times the van der Waals radius of the atoms. Field point charges of −1.0, −0.5, 0.5, and 1.0 *e* are used ($J = 4$). The number of field point charge places (K) of methanol is 110. The one-electron potential change by the polarization is estimated on the same positions of field point charges: the number of the estimated points (L) equals K.

Two types of locally induced dipoles are considered here: an isotropic induced dipole ($\Delta\mu_{km}^{\mathrm{I}}$) and an anisotropic induced dipole ($\Delta\mu_{km}^{\mathrm{A}}$). The induced dipoles are expanded by power series of the electric fields ($\mathbf{E}_{km}$) at the centers (m) of the dipoles, which are produced by the field point charge, as follows:

$$\Delta\mu_{km}^{\mathrm{I}} = \Delta q_{km}^{\mathrm{I}}\mathbf{r}_{m^1} - \Delta q_{km}^{\mathrm{I}}\mathbf{r}_{m^2} \approx \alpha_{km}^{\mathrm{I}}\mathbf{F}_{km} + \frac{1}{2}\beta_{\mathrm{m}}^{\mathrm{I}}(\mathbf{F}_{km})^2$$

$$\Delta\mu_{km}^{\mathrm{A}} = \Delta q_{km}^{\mathrm{A}}\mathbf{r}_{m^a} - \Delta q_{km}^{\mathrm{A}}\mathbf{r}_{m^b} \approx \alpha_{\mathrm{m}}^{\mathrm{A}}(\mathbf{F}_{km}\cos\theta_{km}) + \frac{1}{2}\beta_{\mathrm{m}}^{A}(\mathbf{F}_{km}\cos\theta_{km})^2 \tag{13}$$

where $\Delta q_{km}^{\mathrm{I}}$ and $\Delta q_{km}^{\mathrm{A}}$ are the point charges representing the isotropic and anisotropic induced dipoles, respectively, and $\mathbf{r}_{m^1}$, $\mathbf{r}_{m^2}$, $\mathbf{r}_{m^a}$, and $\mathbf{r}_{m^b}$ are the positional vectors of the locally induced dipoles. α and β denote multicenter polarizability and multicenter first-hyperpolarizability, respectively, and θ_{km} is an angle between the electric field vector and the bond direction. Since the energetic contribution of hyperpolarizabilities is expected to be negligible in molecular interactions, the higher order hyperpolarizabilities are truncated in eq 13. α and β are the optimization parameters of eq 12. For the isotropic induced dipole moments, $|\mathbf{r}_{m^1} - \mathbf{r}_{m^2}|$ is set to 1.0 bohr. For the anisotropic induced dipoles, the bond lengths are used: that is, the induced charges are placed on the atoms of the bond.

The multicenter polarizabilities and first-hyperpolarizabilities of methanol are optimized to reproduce the polarized one-electron potentials obtained from the MP2/6-311++G(2d,2p) wave function. The geometry of methanol is optimized at the Hartree−Fock level. The polarizabilities of ions are also estimated using POP optimization. In the calculations, the van der Waals radii of Cl^-, Na^+, and Mg^{2+} are set to 1.7, 1.57, and 1.36 Å, respectively. All POP optimizations were done by the POPFIT program developed by the author.

The methanol LJ parameters are adopted basically from the pair potentials.[7] Those are adjusted empirically in order to reproduce the ab initio potential energy surfaces of methanol dimer. Preliminary molecular dynamics (MD) simulation of liquid methanol was done using the obtained polarizable model potential in order to test the paramaters. The liquid system consists of 216 molecules in a cubic cell. The periodic boundary condition is employed. The volume of the cell is fixed. The time step is set to 2 fs, and the temperature is kept at 298 K. A production run of 16 ps is carried out. The MD program developed by Torii et al. is used.[49] The LJ parameters of Cl^-, Na^+ and Mg^{2+} are adjusted in order to reproduce the ab initio potential energy surfaces of ion−methanol complexes.

All of the ab initio MO calculations are done with the Gaussian92 computer program.[50]

Interaction Energy Analysis. Quantum mechanical interaction energy between molecules A and B (ΔE_{AB}) is defined as follows:

$$\Delta E_{\mathrm{AB}} = E_{\mathrm{AB}} - E_{\mathrm{A}} - E_{\mathrm{B}} \tag{14}$$

where E_{AB} is the total energy of the A−B complex, and E_{A} and E_{B} are the total energies of the monomer state. Since the difference between the MP2 and SCF interaction energies is defined as the dispersion energy (ΔE_{disp}), the MP2 interaction energy is expressed as follows:

$$\Delta E_{\mathrm{AB}}^{MP2} = \Delta E_{\mathrm{AB}}^{\mathrm{SCF}} + \Delta E_{\mathrm{disp}} \tag{15}$$

There are two types of interaction energy estimations. The first one (ΔE_{AB}) includes the deformation energy of each molecules induced by the complex formation. The optimized energies of the monomer state are used in the interaction energy estimations. The second one (ΔE_{std}) is a standard estimation. The geometry of the complex state is used for the energy estimation of monomers. The difference between ΔE_{AB} and ΔE_{std} is defined as the deformation energy (ΔE_{def}). When we take into account the deformation energies of the SCF level, the MP2 interaction energy is expressed as follows:

$$\Delta E_{\mathrm{AB}}^{\mathrm{MP2}} = \Delta E_{\mathrm{std}}^{\mathrm{SCF}} + \Delta E_{\mathrm{def}}^{\mathrm{SCF}} + \Delta E_{\mathrm{disp}} \tag{16}$$

The standard interaction energy can be decomposed further using energy decomposition analysis (EDA).[51,52] The interaction energies are conventionally decomposed into electrostatic (ES), exchange repulsion (EX), polarization (PLX), charge transfer (CT), and the residual term (R). Thus, the MP2 interaction energy is decomposed as follows:

$$\Delta E_{\mathrm{AB}}^{MP2} = \mathrm{ES} + \mathrm{EX} + \mathrm{PLX} + \mathrm{CT} + \mathrm{R} + \Delta\mathrm{E}_{\mathrm{def}}^{\mathrm{SCF}} + \Delta E_{\mathrm{disp}} \tag{17}$$

For the analysis of PLX and CT, a set of orthogonal molecular orbitals is used, to avoid violating the Pauli exclusion principle, which is violated in the original Kitaura−Morokuma energy decomposition approach.[51] The EDA calculations are carried out using a local version of Gaussian88.[52]

The classical electrostatic energies (E_{es}) are compared with the ES component of EDA. The classical polarization energies (E_{pol}) are compared with the induction energy components (PLX, CT, and R) of EDA. The classical van der Waals energies ($\mathrm{E}_{\mathrm{vdw}}$) are compared with the sum of EX, ΔE_{def}, and ΔE_{disp}.

Results and Discussion

Fractional Point-Charge Parameters. The fractional point-charges of methanol were derived from the ESP optimization. MP2/6-311++G(2d,2p) was used for the calculations of reference electrostatic potentials. Here, two models were adopted. The first is a six-charge model, in which fractional charges are placed on each atom. The second is an eight-charge model. In addition to the six atomic charges, two charges are placed on the centers of the O−H and O−C bonds. Methanol has one methyl hydrogen lying in the Cs plane, and it has the other two methyl hydrogens symmetrically on either side of the Cs plane.

TABLE 1: Fractional Point Charges and Dipole Moments of Methanol

model	six-charge	eight-charge
	Fractional Charge[a]	
O	−0.484	−0.202
H(O)	0.341	0.837
C	−0.097	−0.541
H(C)	0.080	0.142
M(O−C)[b]		0.475
M(O−H)		−0.995
ESP rms deviation[c]	1.6	0.6
percent deviation	23.0	8.7
	Dipole Moment[d]	
ESP fit	1.66	1.75
ab initio	1.72	
experiment	1.69[e], 1.77[f]	

[a] ln *e*. [b] M denotes center of bond. [c] In kcal/mol. [d] In debye. [e] Reference 53. [f] Taken from Table VII of ref 45.

Although those two types of hydrogen are electronically different, the same charges are assigned in the optimization process. Such invariant treatment by the rotation of methyl group is necessary for a force field development.

The optimized charges are shown in Table 1. The eight-charge model shows better optimization results than the six-charge model. The electrostatic potentials are improved significantly by the two additional charges. The charge distribution is usually represented by atomic charges, whereas the distribution of molecules having lone pair electrons, such as water and methanol, is not represented fully. In the latter case the charge distribution is adequately represented by the two additional point charges on the bonds. The calculated dipole moments of the six-charge and eight-charge model are close to the ab initio value using MP2/6-311++G(2d,2p). The ab initio dipole moment reproduces well the experimental values.[45,53] The six-charge and eight-charge models are used in the calculations with the PMP function. Point charge parameters of Cl^-, Na^+, and Mg^{2+} are set to −1, 1, and 2 *e*, respectively.

Multicenter Dipole Polarizability Parameters. The multicenter dipole polarizabilities and first-hyperpolarizabilities of methanol are determined by the POP optimization. Two models (a and ab) are adopted. Model a is an atomic polarization model, in which six induced dipoles are placed on the methanol atoms.

TABLE 2: Multicenter Polarizabilities of Methanol and Polarizabilities of Ions

	Methanol					
	model a		model ab			
	α	$\beta/2^b$	α	$\beta/2^b$	additive[a]	interaction[a]
	Multicenter Polarizabilities[c]					
O	5.02	17.4	4.79	17	4.08	3.14
H(O)	1.52	5.0	1.33	5.9	2.73	0.91
C	4.89	−25.3	−2.06	−53.3	6.93	5.93
H(C)	2.49	14.4	2.48	12	2.75	0.91
O−C			8.3	79.8		
O−H			1.71	1.8		
C−H			5.07	37.2		
POP rms deviation[d]	1.1	0.9	0.7	0.4		
percent deviation	21.7	18.2	12.9	7.1		
	Molecular Polarizability[c]					
CPHF	19.2					
experiment[e]	21.6, 21.8, 22.0					

	Ion		
	Cl^-	Na^+	Mg^{2+}
POP polarizability[c]	18.97	0.75	0.29
POP rms deviation[d]	0.0	0.0	0.5
percent deviation	2.2	2.4	10.1
polarizability[c]			
CPHF	18.0	0.82	0.30
experiment[f]	24.9, 23.3	1.22, 1.27	0.64, 0.07

[a] Reference 30. [b] Multicenter first-hyperpolarizabilities in au. [c] In au. [d] In kcal/mol. [e] Taken from Table II of ref 54. [f] Estimated polarizabilities of Pauling and Fajans are taken from Tables II and IV of ref 55.

Model ab is the combined model of atomic and bond polarization. In addition to the six atomic induced dipoles, five induced dipoles are placed along bonds. MP2/6-311++G(2d,2p) was used for the calculations of polarized one-electron potentials.

The results of POP optimization are shown in Table 2. Model ab shows better results than model a. The relative rms deviations from the ab initio potentials are improved 10% by the additional bond polarizabilities. The contribution of first-hyperpolarizabilities is about 5%. The first-hyperpolarizabilities are neglected in the following interaction energy calculations, because the contribution is small.

TABLE 3: Comparison of the Calculated and Experimental Binding Energies[a]

calculation level single point// geometric optimization	geometry[b]	ΔE_{AB}^{MP2}	ΔE_{AB}^{MP2} (w/ZPEC[c])	ΔE_{std}^{MP2}	ΔE_{std}^{MP2} (w/BSSE)	ΔE_{AB}^{MP2} (w/BSSE, ZPEC[c])	ΔH (experiment)
methanol−methanol							
MP2/6-311++G(2d,2p)// HF/6-31++G(d,p)	*r*(O−O) 2.97	−6.0	−4.7	−5.9	−5.0	−3.7	−3.2 ± 0.1[d]
	a(O−H−O) 177.7						
Cl^-−methanol							
MP2/6-311++G(2d,2p)// HF/6-311++G(2d,2p)	*r*(Cl−H) 2.30	−16.1	−15.3	−16.1	−14.6	−13.7	−17.1 ± 0.1[e]
MP2/6-311++G(d,p)// HF/6-311++G(2d,2p)	*a*(Cl−H−O) 167.1	−16.2	−15.4	−16.1	−13.6	−12.8	
Na^+−methanol							
MP2/6-311++G(2d,2p)// HF/6-311++G(2d,2p)	*r*(Na−O) 2.22	−24.8	−23.8	−24.7	−24.1	−23.1	−26.6[f]
MP2/6-311++G(2d,2p)// HF/6-31++G(d,p)	*a*(Na−O−H)122.3	−26.1	−25.0	−26.1	−24.7	−23.7	
Mg^{2+}−methanol							
MP2/6-311++G(2d,2p)// HF/6-311++G(2d,2p)	*r*(Mg−O) 1.88	−90.8	−89.6	−93.4	−92.4	−88.6	
MP2/6-311++G(d,p)// HF/6-311++G(2d,2p)	*a*(Mg−O−H)121.6	−90.5	−89.3	−93.6	−90.9	−86.6	

[a] In kcal/mol. [b] In angstroms and degrees. [c] HF/6-31++G(d,p) is used for zero-point energy correction. [d] Reference 57. [e] Reference 58. [f] Reference 59.

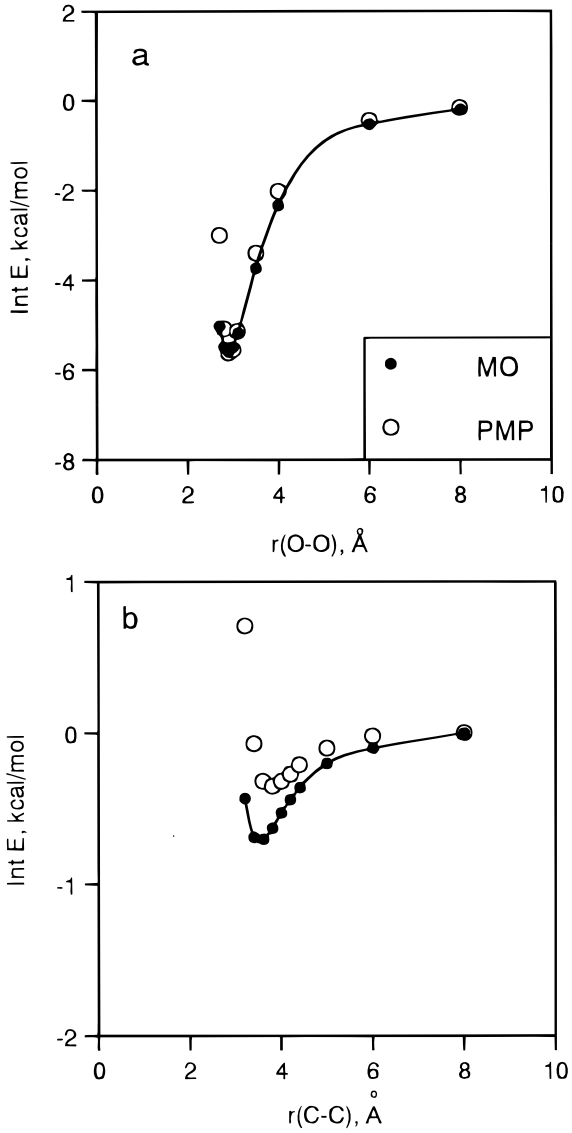

Figure 1. Ab initio MO potential and PMP energy surfaces of methanol dimer: (a) hydrogen bond model, (b) methyl group approach model.

The dipole polarizabilities are estimated using the CPHF method. The calculated mean polarizability of MP2/6-311++G-(2d,2p) underestimates slightly the experimental value (Table 2).[54] Thus, it is anticipated that the multicenter polarizabilities estimated using the MP2/6-311++G(2d,2p) underestimate slightly the experimental value, too.

The POP optimization results of chloride, sodium and magnesium ions are also shown in Table 2. The calculated values reproduce well the polarizabilities derived from CPHF method, whereas these underestimate slightly the experimental values.[55]

Dimerization Energy and Lennard-Jones Parameters To determine LJ parameters, the dimerization energy of methanol is estimated using MP2/6-311++G(2d,2p). The geometry of methanol dimer is optimized using HF/6-31++G(d,p). The computed O−O separation (2.99 Å) corresponds well to an experimental equilibrium distance of 2.98 Å.[56] The dimerization energy is shown in Table 3. The interaction energy of the MP2 level is −6.0 kcal/mol. Zero-point energy correction (ZPEC) is estimated to be 1.3 kcal/mol in the HF level. From the comparison between ΔE_{AB}^{MP2} and ΔE_{std}^{MP2}, it can be seen that there is little deformation of methanol molecules by the complex formation. Corrections for basis-set superposition error (BSSE) have been estimated using the counterpoise procedure. The BSSE is 0.9 kcal/mol. After the correction for the zero-point energy and the BSSE is made, the energy (−3.7 kcal/mol) is comparable with the experimental value derived from infrared pre-dissociation measurements (-3.2 ± 0.1 kcal/mol).[57] Since the corrected value shows good agreement with the experiment, the energy estimation using MP2/6-311++G(2d,2p) is thought to be reliable.

TABLE 4: Van der Waals Parameters

	$2R^*_i$		ϵ_i	
	PMP	published	PMP	published
O	3.10	3.442,[a] 3.446[b]	0.15	0.2104[a], 0.105[b]
H(O)	2.00	0.0,[a] 1.515[b]	0.05	0.0[a], 0.015[b]
C	4.12	3.816,[a] 3.929[b]	0.08	0.1094[a], 0.080[b]
H(C)	2.60	2.774,[a] 2.862[b]	0.02	0.0157[a], 0.022[b]
		Ion		
Cl^-	4.36	4.36−5.46[c]	0.10	0.0401−1.09[c]
Na^+	3.34	2.13−3.74[c]	0.058	0.00277−1.61[c]
Mg^{2+}	1.92	2.32,[d] 1.846[e]	11.00	0.05[d], 0.875[e]

[a] Reference 28. [b] Reference 29. [c] Taken from Table 1 of ref 60. [d] Reference 18. [e] R^*_i and ϵ_i are converted from the A and B constants reported in ref 61.

The vdw parameters of methanol are taken from the LJ parameters of pair potentials[7] and are adjusted in order to reproduce the ab initio potential energy surfaces of methanol dimer. The O and H parameters of alcohol group are adjusted using a model in which a hydrogen bond is formed between alcohol groups of methanol molecules. The parameters of methyl C and H are adjusted using a model in which the methyl groups are close together.

The ab initio radial potential energy surfaces of methanol dimer are calculated. The ΔE_{AB}^{MP2} surfaces of the hydrogen bond model and of the methyl group approach model are shown as lines with closed circles in Figure 1a and Figure 1b, respectively. Here, a O−O length, a linearity of O−H···O and a Cs symmetry were frozen during the geometry optimization of the hydrogen bond model. A C−C length, a linearity of C−C···C−C and a Cs symmetry were frozen during the geometry optimization of the methyl group approach model. The dimerization energy is estimated to be −5.6 kcal/mol (Figure 1a). In the methyl group approach model, a shallow potential minimum of −0.7 kcal/mol, which cannot be observed in the calculations of HF level, is found at the MP2 level (Figure 1b).

The LJ parameters of methanol atoms are optimized in order to reproduce the ab initio potential energy minimums shown in Figure 1a and 1b. In the energy estimations using PMP function, the eight-charge model is used for electrostatic energies. The adjustments of the LJ parameters were made empirically. The optimized LJ parameters are shown in Table 4.

The open circles in Figure 1 show the results calculated by the PMP function. The dimerization energy is −5.6 kcal/mol (Figure 1a). The O−O distance of the hydrogen bond is 2.9 Å. The dimerization energy and hydrogen bond distance are reproduced well by the PMP function. Those of other polarizable potential functions are close to the result of PMP function: −5.56 kcal/mol and 2.75 Å in polarizable intermolecular potential function of Gao[29] and −5.7 kcal/mol and 2.79 Å in the q88 model of Kollman.[28] Those values are smaller and longer, respectively, than pair additive OPLS (optimized potentials for liquid simulations) (−6.80 kcal/mol and 2.73 Å).[29] Such dimerization energy discrepancies between the nonadditive and additive potentials occur, because many-body effects in the liquid state are included implicitly in the OPLS parameters.

In the methyl group approach model, a shallow potential minimum of −0.4 kcal/mol is found in PMP function (Figure 1b). The minimum energy reproduced well the MP2 results.

To test the quality of LJ parameters, preliminary molecular dynamics simulation of methanol liquid is performed using the PMP function determined here. The calculated heat of vaporization in eight-charge model with the atomic polarizabilities was 10.5 kcal/mol. The value overestimates the experimental value of 8.94 kcal/mol.[28,29] Since the heat of vaporization is greatly affected by small changes in the R^* and ϵ parameters, the reproduction of experimental value might be possible by further small adjustment of the parameters.

Reproducibility in Ion−Methanol and Methanol−Ion−Methanol Systems. The reproducibility of interaction energy surfaces under the strong charge field induced by an ion is investigated. First, to show the reliability of reference ab initio MO calculations, the interaction energies of optimized structures are estimated and are compared with the experimental values. The ab initio interaction energies of ion−methanol systems are shown in Table 3. The complex structures are optimized using HF/6-311++G(d,p) and the single-point calculations are performed at the MP2/6-311++G(2d,2p) and MP2/6-311++G(d,p) levels. The interaction energy differences on the basis sets are small in Cl^- and Mg^{2+} complexes. In Na^+ complex the difference is 1.3 kcal/mol.

In the Cl−methanol complex the interaction energy is −16 kcal/mol. The deformation energy is little and the BSSE is 1.5 kcal/mol. The zero-point energy correction in the HF level is 0.8 kcal/mol. The BSSE uncorrected interaction energy is rather close to the experimental value.[58] In the Na^+−methanol complex, the interaction energy is −25 kcal/mol. The deformation energy and the BSSE are small. The zero-point energy correction in the HF level is 1.0 kcal/mol. The interaction energy is expected to underestimate 3 kcal/mol.[59] In the Mg^{2+}−methanol complex the interaction energy is −91 kcal/mol. The deformation energy is −2.6 kcal/mol and the BSSE is 1 kcal/mol. Since the BSSE of ion−methanol systems are fairly small in comparison with the total interaction energies, the correction is not applied in the following calculations of interaction energy surfaces.

The reference ab initio radial potential energy surface scans of ion−methanol systems are shown in Figure 2. The ab initio calculations are performed using MP2/6-311++G(2d,2p). The PMP results accompanied by eight charges and atomic polarizabilities are also shown. The LJ parameters of three ions are optimized in order to reproduce the potential energy minimum. The ab initio interaction energies, shown as a line with closed circles, are well reproduced by the PMP function, shown as open circles. The optimized LJ parameters of ions are shown in Table 4.

So far a wide range of LJ parameter values has been reported for Na^+ and Cl^-.[18,60,61] The PMP parameters reported here are within those reported ranges (Table 4). The R^* parameter of Mg^{2+} was within the range of reported values, whereas the ϵ parameter of Mg^{2+} showed a relatively deep well.

The reproducibility of interaction energy surfaces of methanol−ion−methanol systems were investigated. After the systems were geometrically optimized using HF/6-31++G(d,p), the interaction energies were estimated using MP2/6-311++G(d,p). The potential energy surfaces for the three ions are presented in Figure 2. The results of the reference ab initio potential surfaces are shown in the lines with closed squares. The results of PMP function are presented as the open squares. The ab initio surfaces

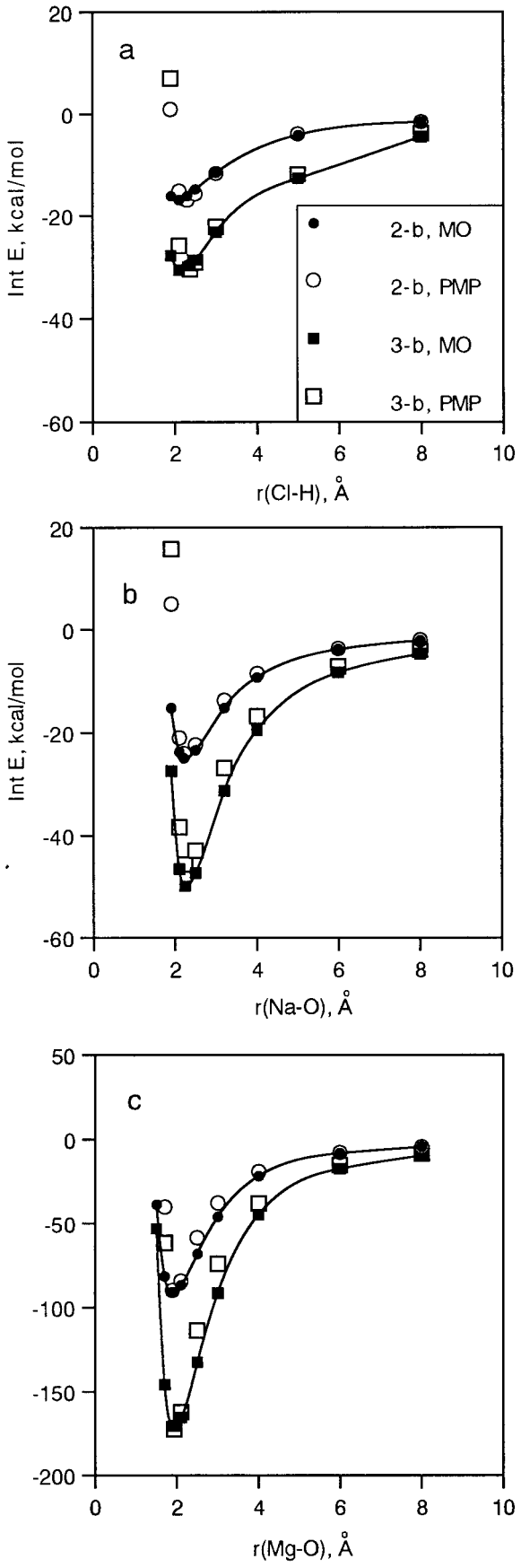

Figure 2. Ab initio MO potential and PMP energy surfaces of ion−methanol two-body (2-b) and methanol−ion−methanol three-body (3-b) system: (a) Cl^-−methanol and methanol−Cl^-−methanol, (b) Na^+−methanol and methanol−Na^+−methanol, (c) Mg^{2+}−methanol and methanol−Mg^{2+}−methanol.

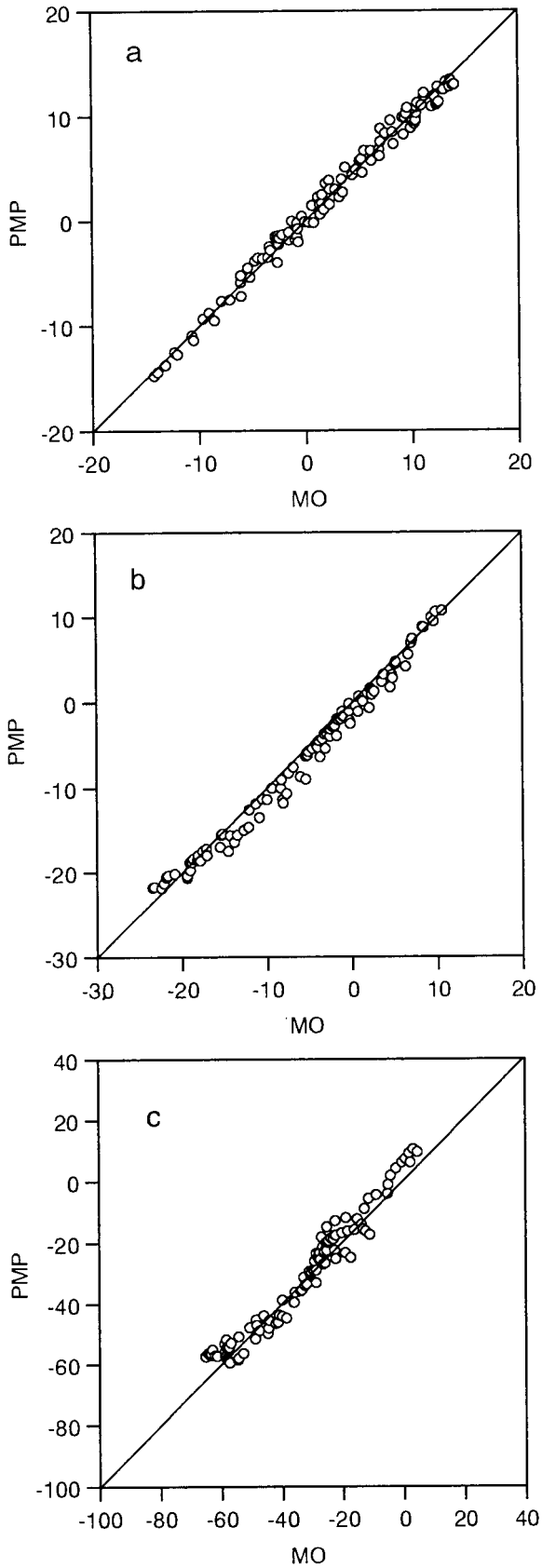

Figure 3. Comparison of ion−methanol interaction energies (kcal/mol) between ab initio MO potential and PMP function at various sampling configurations: (a) Cl^-−methanol, (b) Na^+−methanol, (c) Mg^{2+}−methanol.

are reproduced well by the PMP function. It is expected that the PMP function can handle the most of the many-body effects.

Furthermore, the various configurations are tested using the ion−methanol complexes. In the Cl^-−methanol complexes, a Cl^- is placed in the various positions on the surface of two times of van der Waals radius of methanol atoms. In the Na^+−methanol and Mg^{2+}−methanol complexes, an ion is placed on the surface of 1.8 times of van der Waals radius, since these radii are smaller than that of Cl^-. Here, the reference ab initio calculation level is MP2/6-311++G(d,p). In Figure 3 the interaction energy results are compared with those from the ab initio molecular orbital calculations. In the three systems, good correspondences are found in both attractive and repulsive wide energy regions.

TABLE 5: Average Root-Mean-Square Deviations from ab Initio Interaction Energies

charge model	polarization model	Cl^-−methanol	Na^+−methanol	Mg^{2+}−methanol
six	a	2.3[a] [28][b]	2.3 [21]	6.3 [17]
six	ab	2.2 [29]	2.4 [22]	5.3 [14]
eight	a	0.7 [10]	1.4 [12]	4.5 [12]
eight	ab	0.8 [9]	1.7 [15]	3.3 [9]
eight	additive[c]	1.1 [14]	2.2 [20]	5.3 [14]
eight	interaction[c]	1.8 [23]	1.8 [17]	11.6 [30]

[a] In kcal/mol. [b] Percent deviations are shown in brackets. [c] Reference 30.

TABLE 6: Average Root-Mean-Square Deviations from ab Initio Surface Electrostatic Potentials of Ion−Methanol Complexes

model		system		
charge	polarization	Cl^-−methanol	Na^+−methanol	Mg^{2+}−methanol
six	a	2.3[a] [27][b]	1.9 [2.1]	3.9 [2.0]
six	ab	2.4 [2.8]	1.8 [2.0]	3.4 [1.7]
eight	a	1.8 [2.1]	1.2 [1.4]	3.6 [1.8]
eight	ab	1.8 [2.1]	1.1 [1.2]	3.0 [1.5]
six		3.5 [4.0]	4.9 [5.4]	12.6 [6.4]
eight		3.4 [3.9]	4.5 [5.0]	12.4 [6.3]
ESP fitting charge		1.2 [1.4]	1.0 [1.2]	1.7 [0.9]

[a] In kcal/mol. [b] Percent rms deviations are shown in brackets.

TABLE 7: Energy Decomposition Analysis and Classical Interaction Energies of Ion−Methanol System

interaction energy[a]		Cl^-−methanol		Na^+−methanol		Mg^{2+}−methanol	
EDA	PMP	EDA	PMP	EDA	PMP	EDA	PMP
ΔE_{opt}^{MP2}	(E_{tot})	−16.1	(−16.9)	−24.8	(−23.9)	−90.8	(−90.0)
ΔE_{opt}^{SCF}		−12.3		−25.8		−92.7	
ΔE_{std}^{SCF}		−12.6		−26.3		−97.9	
ΔE_{def}		0.3		0.5		5.2	
ΔE_{disp}		−3.8		1.0		1.8	
ES	(E_{es})	−16.2	(−14.2)	−28.3	(−22.4)	−81.8	(−60.7)
EX	(E_{vdw})	9.7	(2.5)	9.0	(6.4)	32.2	(24.7)
PLX	(E_{pol})	−3.1	(−5.2)	−5.3	(−7.9)	−30.7	(−54.0)
CT		−2.3		−0.7		−7.0	
R		−0.7		−1.0		−10.6	

[a] In kcal/mol.

The root-mean-square (rms) deviations of various models from the ab initio interaction energies are shown in Table 5. The results of six-charge and eight-charge model are compared. Clearly the eight-charge model showed better results than the six-charge model. There are little differences between model a and model ab. The percent deviations of the eight-charge model with atomic polarizabilities were within 12%. The atomic polarization model is appropriate for methanol that shows spherical polarization around the atoms by σ-electrons.[45]

Several atomic polarizability models have been reported.[30−32] These are divided into two types. The first type is an additive atom polarizability, in which atom−atom intramolecular interac-

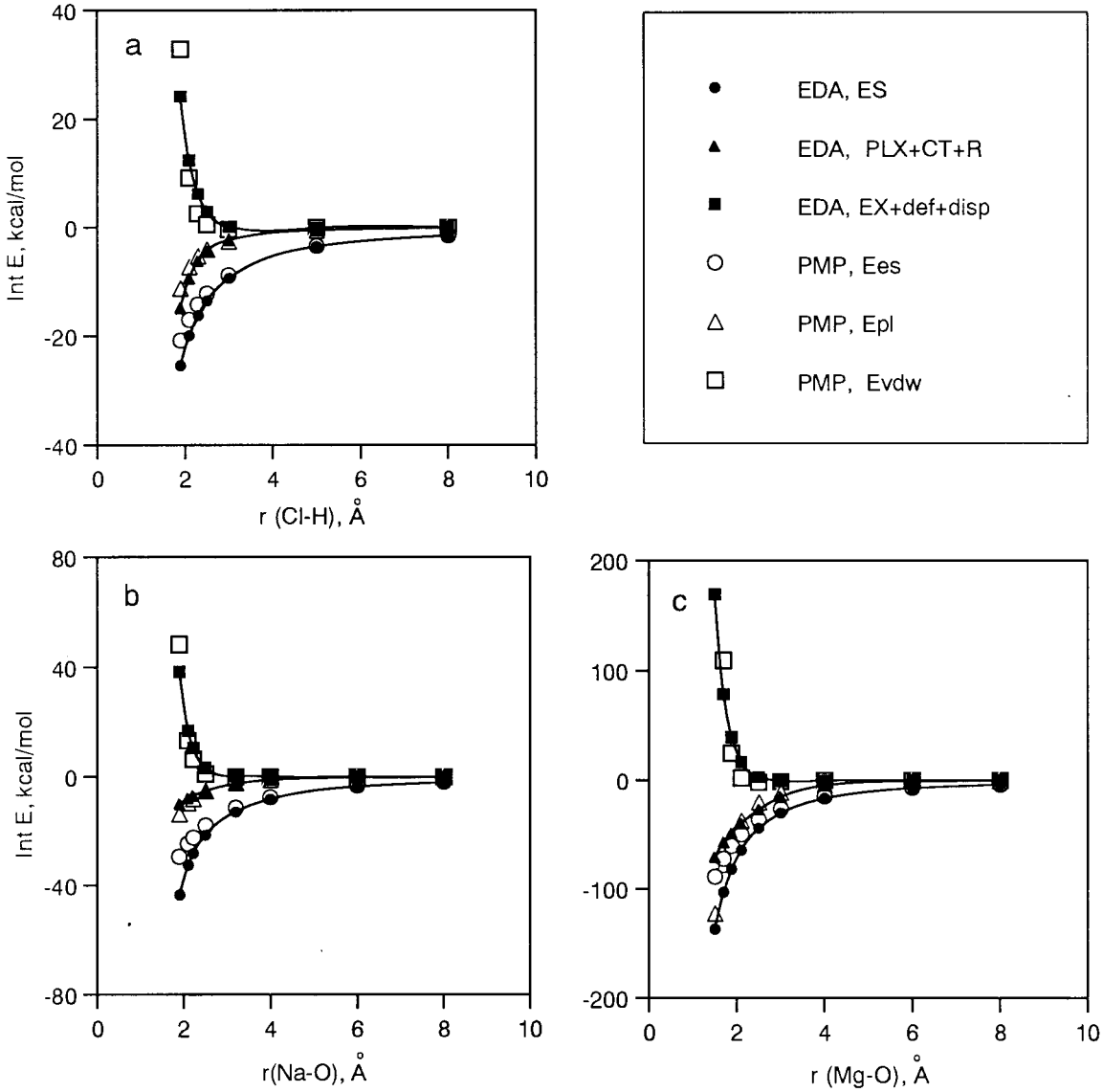

Figure 4. Energy component surfaces of ab initio MO potential and PMP: (a) Cl^-−methanol, (b) Na^+−methanol, (c) Mg^{2+}−methanol.

tion (i.e., charge-inducible dipoles) is not allowed. The polarization treatment of PMP function is same as the additive atom polarizability. The second type is an atom dipole interaction model proposed by Applequist[30] and Thole.[31] The atom−atom intramolecular interaction is allowed in the interaction model. The reported atomic polarizabilities of the additive model and of the interaction model are listed in Table 2. The parameter values of the interaction model are naturally smaller than the additive model. Those parameters with the eight-charge model are used for the interaction energy estimation of ion−methanol systems (Table 5). Relatively good results are obtained in the additive model. In the interaction model, serious underestimation of interaction energy occurs under the strong electric field.

The polarizabilities of the atom dipole interaction model proposed by Applequist et al.[30] have been often used for MD simulations of liquids.[18,19,21,28] Intramolecular polarization interactions between atoms attached by one and two bonds (1−2 and 1−3 interaction) have usually been neglected in these simulations. As deduced from the results of Table 5, such neglect in the atom dipole interaction model brings the underestimation of the polarization energy. Intramolecular 1−2 and 1−3 charge−charge interactions have always been neglected in the evaluations of electrostatic energy. Intramolecular 1−4 charge−charge interactions have often been reduced by half. In the development of the polarizable potential function, the neglect of intramolecular polarization is natural, in line with the treatment of charge−charge intramolecular interaction, and the risk for polarization catastrophe is always avoidable.

Next, the reproducibility of the charge distributions of the ion−methanol systems is studied using the electrostatic potentials on the ion−methanol complex surfaces. The average rms deviations from the reference ab initio electrostatic potentials are shown in Table 6. In the ion−methanol complexes the eight-charge model showed better results than the six-charge model. The average percent deviations of eight-charge model are 1−2%. There are little differences between model a and model ab.

Additionally the rms deviations of two models are calculated. The first one is a nonpolarizable model, in which the polarization term was removed from the PMP function. In the nonpolarizable models the average deviations are 4−6%. The second one is a charge−relaxation model, in which all atomic charges of methanol and ion are relaxed simultaneously during the ESP optimization. In this model the charge transfer between ion and methanol is allowed in addition to the intramolecular polarization. The average deviations are 1% in the charge relax models. Since the results of PMP function are rather close to the charge relaxed model, it is expected that the considerable parts of charge

redistribution are corrected by the introduction of multicenter polarizabilities.

Analysis of Interaction Energy. The energy terms of PMP function are compared with those of ab initio energy decomposition analyses (EDA). The results of ion−methanol complexes are shown in Table 7. The electrostatic energies (E_{es}) underestimate slightly the ES components of EDA. The vdw energies (E_{vdw}) correspond with the sums of EX and ΔE_{disp}. The polarization energies (E_{pol}) overestimate the PLX components of EDA, but those correspond with the sums of PLX, CT, and R of EDA, namely, induction energies.

The analysis results of radial energy surfaces of ion−methanol systems are presented in Figure 4. The electrostatic energy curves of EDA are shown in the lines with closed circles. The electrostatic energies derived from the PMP function are shown as open circles. The electrostatic energies of PMP underestimate the ES components of EDA, especially at short separations. The polarization energies of the PMP function are shown as open triangles, and the induction energies (PLX + CT + R) are shown in lines with closed triangles. In the Na^+−methanol and Mg^{2+}−methanol complex, the overestimation of classical polarization energies is found in the very short separations of ion and methanol. Those might be the beginning of polarization catastrophe. The correspondence between the potential energy curves is good, except for the short-range separations. The classical vdw energies are compared with the sums of exchange repulsion, dispersion and deformation energies. The vdw energies are shown as open squares, and the sums (EX + ΔE_{disp} + ΔE_{def}) are shown as lines with the closed squares. Although the repulsive walls of PMP energy surfaces are too steep in the short distances, the LJ potential properly describes the sums of exchange repulsion, dispersion, and deformation energies. The ϵ parameter of Mg^{2+} was large, as shown in Table 4. From the analysis of Figure 4c it can be seen that the cause comes from the underestimation of classical electrostatic energies rather than the classical polarization energy.

Energy decomposition analyses show that many-body potential can be constructed by the introduction of the atomic polarization term into the pair potentials. Without the introduction of a short-range dumping function for polarization term, the PMP function can reproduce the total potential energy surfaces very well in the ion−methanol systems.

Conclusions

A polarized model potential (PMP) function was developed for ion−methanol system. The characteristics of the PMP function are in the reproducibility of high level ab initio molecular orbital calculations (MP2/6-311++G(2d,2p) level). Although the PMP function consists of only three classical terms (Coulomb, polarization, and van der Waals), the interaction energies and charge distributions of ion−methanol system are reproduced very well. The PMP function is applicable from a neutral system, such as methanol dimer, to highly ionic system such as Mg^{2+}−methanol complex. The PMP function also reproduced well the potential energy surfaces of not only the two-body ion−methanol system but also those of the three-body methanol−ion−methanol system. The PMP function can incorporate adequately the many-body effects.

The origin of each terms of PMP function was clarified by the energy decomposition analysis (EDA). The fractional point charges of methanol reproduced well the electrostatic interaction energy of EDA (ES). The atomic polarizabilities of methanol reproduced well the induction energies of EDA (PL+ CT + R). By the introduction of atomic polarization, the PMP function can respond to wide range external fields, induced by an anion, a cation, or a divalent cation. The van der Waals term well represents the sum of exchange repulsion (EX), dispersion (ΔE_{disp}), and deformation (ΔE_{def}) energies. Although well-known polarization instability occurs in short-range interaction, the excessive attractive energies of polarization are adequately canceled out by the repulsive potential wall of LJ term. Reliable analysis for polarization contribution is possible by using the PMP function.

The parameter derivations by ESP optimization and by POP optimization are straightforward, and those can be applied to any molecules. The LJ parameters of pair potentials are basically used without large modifications for PMP function. Thus, the systematic parametrization of the PMP function opens the way to establish a simple and reliable force field for molecular simulations of large inhomogeneous systems, including monovalent and divalent ions.

Acknowledgment. The author is grateful to the late Professor K. Fukui, Dr. T. Komatsuzaki of University of Kobe, and Dr. H. Torii of University of Tokyo for their helpful discussions. Some parts of this work were performed while the author was at the Institute for Fundamental Chemistry. This work was supported by a Kinjo Gakuin University Special Research Subsidy, and a Kinjo Gakuin University-Parent Teacher Association Special Research Subsidy.

References and Notes

(1) Stillinger, F. H.; Rahman, A. *J. Chem. Phys.* **1974**, *60*, 1545.
(2) Matsuoka, O.; Clementi, E.; Yoshimine, M. *J. Chem. Phys.* **1976**, *64*, 1351.
(3) Berendsen, H. J. C.; Postma, J. P. M.; van Gunsteren, W. F.; Hermas, J. *In Intermolecular Forces*; Pullman, B., Ed.; Reidel: Dordrecht, Holland, 1981; p 331.
(4) Jorgensen, W. L.; Chandrasekhar, J.; Madura, J. D.; Impey, R. W.; Klein, M. L. *J. Chem. Phys.* **1983**, *79*, 926.
(5) Jorgensen, W. L.; Madura, J. D.; Swenson, C. J. *J. Am. Chem. Soc.* **1984**, *106*, 6638.
(6) Jorgensen, W. L. *J. Phys. Chem.* **1986**, *90*, 1276.
(7) Brooks, B. R.; Bruccoleri, R. E.; Olafson, B. D.; States, D. J.; Swaminathan, S.; Karplus, M. *J. Comput. Chem.* **1983**, *4*, 187.
(8) Weiner, S. J.; Kollman, P. A.; Case, D. A.; Singh, U. C.; Chio, C.; Alagona, G.; Profeta, S., Jr.; Weiner, P. *J. Am. Chem. Soc.* **1984**, *106*, 765.
(9) Jorgensen, W. L.; Tirado-Rives, J. *J. Am. Chem. Soc.* **1988**, *110*, 1657.
(10) Barnes, P.; Finney, J. L.; Nicholas, J. D.; Quinn, J. E. *Nature* **1979**, *282*, 459.
(11) Dykstra, C. E. *Chem. Rev.* **1993**, *93*, 2339.
(12) Ahlström, P.; Wallqvist, A.; Engström, S.; Jönsson, B. *Mol. Phys.* **1989**, *68*, 563.
(13) Kozack, R. E.; Jordan, P. C. *J. Chem. Phys.* **1992**, *96*, 3120.
(14) Wallqvist, A.; Berne, B. J. *J. Phys. Chem.* **1993**, *97*, 13841.
(15) Dang, L. X. *J. Phys. Chem.* **1998**, *102*, 620.
(16) Sprik, M.; Klein, M. L. *J. Chem. Phys.* **1988**, *89*, 7556.
(17) Rick, S. W.; Stuart, S. J.; Berne, B. J. *J. Chem. Phys.* **1994**, *101*, 6141.
(18) Lybrand, T. P.; Kollman, P. A. J. *Chem. Phys.* **1985**, *83*, 2923.
(19) Cieplak, P.; Kollman, P.; Lybrand, T. *J. Chem. Phys.* **1990**, *92*, 6755−6760.
(20) Wallqvist, A.; Ahlström, P.; Karlström, G. *J. Phys. Chem.* **1990**, *94*, 1649.
(21) Caldwell, J.; Dang, L. X.; Kollman, P. A. *J. Am. Chem. Soc.* **1990**, *112*, 9144.
(22) Dang, L. X. *J. Chem. Phys.* **1992**, *97*, 2659.
(23) Bernardo, D. N.; Ding, Y.; Krogh-Jespersen, K.; Levy, R. M. *J. Phys. Chem.* **1994**, *98*, 4180.
(24) Clementi, E.; Kistenmacher, H.; Kolos, W.; Romano, S. *Theor. Chim. Acta* **1980**, *55*, 257.
(25) Niesar, U.; Corongiu, G.; Clementi, E.; Kneller, G. R.; Bhattacharya, D. K. *J. Phys. Chem.* **1990**, *94*, 7949.
(26) Skaf, M. S.; Fonseca, T.; Ladanyi, B. M. *J. Chem. Phys.* **1993**, *98*, 8929.
(27) Meng, E. C.; Cieplak, P.; Caldwell, J. W.; Kollman, P. A. *J. Am. Chem. Soc.* **1994**, *116*, 12061.
(28) Caldwell, J. W.; Kollman, P. A. *J. Phys. Chem.* **1995**, *99*, 6208.

(29) Gao, J.; Habibollazadeh, D.; Shao, L. *J. Phys. Chem.* **1995**, *99*, 16460.
(30) Applequist, J.; Carl, J. R.; Fung, K.-K. *J. Am. Chem. Soc.* **1972**, *94*, 2952.
(31) Thole, B. T. *Chem. Phys.* **1981**, *59*, 341.
(32) van Duijnen, P. T.; Swart, M. *J. Phys. Chem.* **1998**, *102*, 2399.
(33) Astrand, P.-O.; Wallqvist, A.; Karlström, G. *J. Chem. Phys.* **1994**, *100*, 1262.
(34) Millot, C.; Soetens, J.-C.; Costa, M. T. C. M.; Hodges, M. P.; Stone, A. J. *J. Phys. Chem. A* **1998**, *102*, 754.
(35) Stone, A. *J. Mol. Phys.* **1985**, *56*, 1065.
(36) Bader, R. F. W.; Keith, T. A.; Gough, K. M.; Laidig, K. E. *Mol. Phys.* **1992**, *75*, 1167.
(37) Garmer, D. R.; Stevens, W. J. *J. Phys. Chem.* **1989**, *93*, 8263.
(38) Voisin, C.; Cartier, A. J. *Mol. Struct.* **1993**, *286*, 35.
(39) Le Sueur, C. R.; Stone, A. J. *Mol. Phys.* **1993**, *78*, 1267.
(40) Ángyán, J. G.; Jansen, G.; Loos, M.; Hättig, C.; Hess, B. A. *Chem. Phys. Lett.* **1994**, *219*, 267.
(41) Soetens, J.-C.; Millot, C.; Chipot, C.; Jansen, G.; Ángyán, J. G.; Maigret, B. *J. Phys. Chem. B* **1997**, *101*, 10910.
(42) Nakagawa, S.; Kosugi, N. *Chem. Phys. Lett.* **1993**, *210*, 180.
(43) Nakagawa, S. *Chem. Phys. Lett.* **1995**, *246*, 256.
(44) Nakagawa, S. *Chem. Phys. Lett.* **1997**, *278*, 272.
(45) Voisin, C.; Cartier, A.; Rivail, J.-L. *J. Phys. Chem.* **1992**, *96*, 7966.
(46) Murphy, W. F. *J. Chem. Phys.* **1977**, *67*, 5877.
(47) Singh, U. C.; Kollman, P. A. *J. Comput. Chem.* **1984**, *5*, 129.
(48) Bayly, C. I.; Cieplak, P.; Cornell, W. D.; Kollman, P. A. *J. Phys. Chem.* **1993**, *97*, 10269.
(49) Torii, H.; Tatsumi, T.; Kanazawa, T.; Tasumi, M. *J. Phys. Chem.* **1998**, *102*, 2, 309.
(50) Frisch, M. J.; Trucks, G. W.; Head-Gordon, M.; Gill, P. M. W.; Wong, M. W.; Foresman, J. B.; Johnson, B. G.; Schlegel, H. B.; Robb, M. A.; Replogle, E. S.; Gomperts, R.; Andres, J. L.; Raghavachari, K.; Binkley, J. S.; Gonzalez, C.; Martin, R. L.; Fox, D. J.; Defrees, D. J.; Baker, J.; Stewart, J. J. P.; Pople, J. A. *Gaussian92*, Revision A; Gaussian, Inc.: Pittsburgh, PA, 1992.
(51) Kitaura, K.; Morokuma, K. *Int. J. Quantum Chem.* **1976**, *10*, 325.
(52) Komatsuzaki, T.; Ohmine, I. *Chem. Phys.* **1994**, *180*, 239.
(53) McClellan, A. L. *Tables of Experimental Dipole Moments*; Freeman and Co.: San Francisico, 1963.
(54) Miller, K. J. *J. Am. Chem. Soc.* **1990**, *112*, 8533.
(55) Coker, H. *J. Phys. Chem.* **1976**, *80*, 2078.
(56) Lovas, F. J.; Belov, S. P.; Tretyakov, M. Y.; Stahl, W.; Suenram, R. D. *J. Mol. Spectrosc.* **1995**, *170*, 478−92.
(57) Bizzarri, A.; Stolte, S.; Reuss, J.; Rijdt, J. G. C. M. V. D.-V. D.; Duijneveldt, F. B. V. *Chem. Phys.* **1990**, *143*, 423.
(58) Evans, D. H.; Keesee, R. G.; Castleman, A. W., Jr. *J. Phys. Chem.* **1991**, *95*, 3558.
(59) Guo, B. C.; Conklin, B. J.; Castleman, A. W., Jr. *J. Am. Chem. Soc.* **1989**, *111*, 6506.
(60) Peng, Z.; Ewig, C. S.; Hwang, M.-J.; Waldman, M.; Hagler, A. T. **1997**, *101*, 7243.
(61) Åqvist, J. J. *Phys. Chem.* **1990**, *94*, 8021.